

# Explaining Residential Electricity Consumption with Satellite Imagery

Simone Fobi

sf2786@columbia.edu

Terence Conlon

tmc2180@columbia.edu

## Abstract

*In this report, we use high resolution imagery and utility-reported data to determine what image features correspond to multiple levels of residential electricity consumption. To do so, we implement a cycle-consistent generative adversarial network; the output of the generative network provides visual understanding about the types of development influence consumption. Results from our work indicate that larger, more visually distinct buildings and roads are the features most correlated with high electricity consumption. To a lesser extent, increased contrast in nearby fields – possibly indicating higher levels of agricultural management – is also linked to higher consumption. We also discuss two extensions made to our generative model. First, we expand on our baseline binary network to create a conditional generative model. Next, we explore methods of using generated images to aid an electricity consumption classification network. Here, we discuss the techniques we tested and their performance relative to the baseline classifiers.*

*The contributions of this paper are threefold. First, we increase domain knowledge about the types of features that correlate with electricity consumption by providing visually interpretable masks. Second, we introduce a cycle-consistent, conditional generative adversarial network architecture that can be used for unpaired image translation among a set of classes. Lastly, we discuss the utility of generated imagery in pursuing other research questions, namely the development of a network that classifies satellite imagery according to electricity consumption.*

## 1. Introduction

Electricity services have historically been provided through grid extension efforts, whereby a centralized electricity network is expanded to connect new customers. However, in developing countries, the cost of grid extension increases significantly when connecting customers distant from the central grid; typically found in highly rural setting, these customers tend to consume less electricity than those connected previously [4]. As a result, electric utilities struggle to recover the cost of grid extension for re-

mote customers, making it harder to provide electricity access throughout the country.

Despite the structural challenges associated with electrification efforts, improvements in distributed energy systems, mobile payment platforms, and grid data management have driven recent gains in increasing electricity access. Governments and entrepreneurs are exploring new pathways for electrification such as solar home systems and minigrids, as well as redoubling investments in traditional grid extension, all in an effort to improve livelihoods and build sustainable institutions for delivering electricity services. An area that remains a challenge in this space is determining the relevant characteristics of an area that influence its electricity consumption. If utilities can understand what types of development drive consumption, this knowledge can help planners design generation and distribution systems to deliver power at the lowest cost. Moreover, in grid-connected regions where reliable, frequent consumption data is unavailable, either because this information has been lost on its way back to the utility, or because interested parties do not have access to proprietary records, an understanding of the features that influence consumption can help researchers and analysts infill consumption estimates.

Over the past decade, there has been tremendous growth in the volume of and access to global satellite imagery, growth which has been fueled by the deployment of cheaper, faster satellites into orbit [7]. Remote sensed data has been leveraged to understand drivers for economic growth and development, which in turn is correlated with electricity consumption [16], [10]. By pairing satellite imagery, available over a wide swath of the globe, with more sparse electricity consumption averages, we can discern relationships between the two data sources in order to understand consumption patterns for images where labels are unavailable [1].

Independently, generative adversarial networks (GANs) are becoming increasingly popular for exploring the exact nature of a decision boundary in classification problems [5]. Traditional GANs alternate training a classifier and a discriminator in order to generate images indistinguishable from those in a target set. Here, we use a GAN variant – a CycleGAN [17] – to implement unpaired image-to-image

translation between classes of images that correspond to various levels of monthly electricity consumption. Generative networks allow us to create visual features that are both important in differentiating between images in different electricity consumption classes and also general across an entire set of images, unlike insights gained from image-specific, classification network heatmap analysis.

In this project, we help answer the question of what features are present in high and low electricity consumption images. Presented visually, this understanding will increase domain knowledge about what types of development correspond to higher electricity consumption. Furthermore, we attempt to show the application of generated imagery to the field of electricity system planning. Computer vision researchers have made significant progress in the image generation field in recent years, however these advances have mostly found application in related, academic contexts. If these advanced techniques can be applied to another technical domain, our work can provide justification for further knowledge transfer across disciplines.

## 2. Related Work

Multiple projects have leveraged satellite images to answer various questions on land use, road quality and consumption expenditure: by linking sparse ground-truth with abundant imagery, researchers can extrapolate trends in existing data to areas where labelled data exists [13], [3]. Jean et al. combine Google maps daytime images (provided by DigitalGlobe), nighttime lighting, and survey data to estimate poverty for multiple African countries [9]. High resolution daytime images were used to train a model to predict nighttime lights as measured by DMSP-OLS; features extracted from the last layer of the model were then used to estimate household expenditure or wealth. Results from this paper suggest that there are important features about economic development which can be gleaned from remote sensed data. Further work on this topic has incorporated artificially generated imagery to improve the poverty predictions [11]. While these following results are inconclusive, this recent report indicates that researchers believe generated images can help a classifier network better generalize to unseen landscapes.

GANs can be used to identify and visualize features that impact classification decisions, as they allow a user to inspect how the addition of certain feature vectors cause an image to fall on the other side of a decision boundary [15]. A certain subset of GANs deal with unpaired image-to-image translation, whereby an image from one class is changed into another class without the generation network knowing exactly what the transformed image should look like; the network is trained to pick out general characteristics of the sets of images in question, and apply these characteristics to an image to transform from it from one class to

another. We use the CycleGAN variant introduced in [17] to learn features salient in classifying low and high electricity consumption images.

Separately, [14] and [12] propose methods to stabilize GAN training, techniques which have proved valuable in dealing with satellite imagery that often has a high ratio of background to foreground image features. Further extensions in the image-to-image translation space include [8] and [6], papers which introduce the concept of conditional GANs; these networks take in a target class as an additional input and generate an image in this class accordingly. In generating images in multiple electricity consumption classes, we recreate this conditional GAN framework.

## 3. Data

Average monthly electricity consumption data for this report comes from Kenya Power and Lighting Company (KPLC), the sole utility operating in Kenya. We use reported consumption quantities from 2013 in order to pair the consumption with available satellite imagery taken during the same year. Satellite imagery for this project comes from DigitalGlobe. The DigitalGlobe imagery has 3 bands (RGB) and a resolution of approximately 0.48 meters per pixel. All images are clipped to a height and width of 450m, as this spatial extent corresponds to the resolution of the nighttime light measurements provided by DMSP-OLS, data used to create a baseline electricity classification model. Only image patches that contain residential electricity consumers with measured monthly data – as determined by coordinates associated with each the consumers – are considered as model inputs. At this point, we have a set of 450m by 450m images, each with an associated consumption metric, calculated as the average of all monthly consumption quantities for every consumer with reported data in the image. It is important to note that not all households in the image have an electric connection. In addition, as we only have a sample of consumption for the country, there are electricity customers in the image for whom we don't have consumption data.

We further pare down the image set with coupled consumption quantities by considering only image patches with consumption that falls in set electricity consumption classes. Here, in determining the most appropriate class boundaries, we first evaluated the relative distribution of average monthly consumption quantities for all image patches with reported monthly consumption. We constrain the low-consumption class to contain 2915 images with consumption between 3 kWh/month and 30 kWh/month; the medium-consumption class consists of 2874 images that contain residential consumers that average between 40 kWh/month and 70 kWh/month; the high-consumption class contains 2914 images with consumption between 90 kWh/month and 1000 kWh/month. Here, the three con-

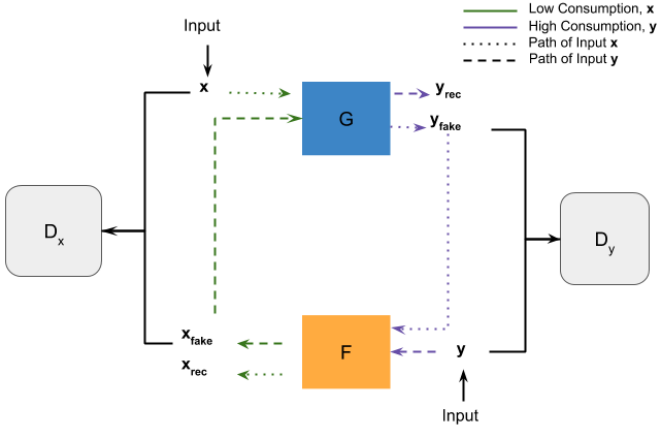


Figure 1: Binary CycleGAN architecture. Input images of class  $X$  and class  $Y$  are given as inputs; the model alternately trains the generators  $\mathbf{G}$  and  $\mathbf{F}$  and the discriminators  $\mathbf{D}_X$  and  $\mathbf{D}_Y$  in order to generate better fake images  $y_{fake}$  and  $x_{fake}$ .

sumption classes correspond to consumption values likely to be found in rural, periurban, and urban settings. The high-consumption and low-consumption classes are used in the binary CycleGAN implementation, while images from all three classes are used in the conditional CycleGAN implementation. A training ratio of 0.7 is used for all three classes.

## 4. Methodology

### 4.1. Binary CycleGAN Implementation

We adapt the structure for our binary CycleGAN from the original CycleGAN implementation in [17]. The model architecture for this implementation is shown in Figure 1. Here, images of class  $X$  (low consumption) and  $Y$  (high consumption) are given as inputs to generators  $\mathbf{G}$  and  $\mathbf{F}$ , respectively. The generated images ( $y_{fake}$ ,  $x_{fake}$ ) are both sent to their respective discriminators ( $\mathbf{D}_X$  and  $\mathbf{D}_Y$ ), where they are compared to real images in class  $X$  and  $Y$  to quantify the adversarial loss. The generated images are also sent back through the opposing generator ( $\mathbf{F}$  and  $\mathbf{G}$ , respectively) to recreate images of the original class. The recreated images ( $y_{rec}$ ,  $x_{rec}$ ) are compared to the original  $x$  and  $y$  images to attain the cycle-consistency loss. During training, these losses – the adversarial loss and the cycle consistency loss – are used to update the weights in the discriminator and generator.

However, in order to achieve the best model performance, a couple key changes to the baseline are necessary. In training and validation, all images are randomly cropped to a size of (472,472,3), as the model generators and discriminators have difficulty processing images at the origi-

nal size of (930,930,3). We also implemented a number of custom losses not present in the original CycleGAN baseline. Along with the adversarial loss ( $L_{gan}$ , generator and discriminator loss combined) and the cycle consistency loss ( $L_{cyc}$ ), both explained in [17], our network enforces a class maximizing loss and an illumination loss. The class maximizing loss ensures that in transforming an image across the decision boundary, generated images are perceptibly different from their original inputs; in practice, this loss works as a helpful counterbalance to the cycle consistency loss, similar to how the two parts of the generator and discriminator losses act adversarially. The model's final loss, the illumination loss, ensures that any global change in the pixel values is kept minimal. Because electricity consumption is closely intertwined with development, overall image hue can mirror electricity consumption: images that contain low consumption are often more rural and therefore more green, while images with higher consumption are more urbanized and less green. Therefore, the illumination loss prevents the CycleGAN from merely increasing or decreasing the greenness to generate alternate-class images, instead incentivizing local, distinct image changes. All losses are shown in equation form below:

$$\begin{aligned} L_{gan}(G, D_y, X, Y) = & \lambda_1 * \mathbb{E}_{y \sim p_{data}(y)} [\log(D_y(y))] + \\ & \lambda_2 * \mathbb{E}_{x \sim p_{data}(x)} [\log(1 - D_y(G(x))] \end{aligned} \quad (1)$$

$$\begin{aligned} L_{cyc}(G, F, X, Y) = & \lambda_3 * (\mathbb{E}_{x \sim p_{data}(x)} [|F(G(x)) - x|] + \\ & \mathbb{E}_{y \sim p_{data}(y)} [|G(F(y)) - y|]) \end{aligned} \quad (2)$$

$$\begin{aligned} L_{cmax}(G, F, X, Y) = & -\lambda_4 * (\mathbb{E}_{x \sim p_{data}(x)} [|G(x) - x|] + \\ & \mathbb{E}_{y \sim p_{data}(y)} [|F(y) - y|]) \end{aligned} \quad (3)$$

$$\begin{aligned} L_{illum}(G, F, X, Y) = & \lambda_5 * (\sum \mathbb{E}_{x \sim p_{data}(x)} [|G(x) - x|] + \\ & \sum \mathbb{E}_{y \sim p_{data}(y)} [|F(y) - y|]) \end{aligned} \quad (4)$$

$$\begin{aligned} L_{total} = & L_{gan}(G, D_y, X, Y) + L_{gan}(F, D_x, X, Y) + \\ & L_{cyc}(G, F, X, Y) + L_{cmax}(G, F, X, Y) + \\ & L_{illum}(G, F, X, Y) \end{aligned} \quad (5)$$

In practice, we found that loss weights of  $\lambda_1 = 10$ ,  $\lambda_2 = 1$ ,  $\lambda_3 = 10$ ,  $\lambda_4 = 5$ ,  $\lambda_5 = 66.8$  allow for the best performance. We also used other GAN training tips to reach model stability, including: label switching at a rate of 0.2; using soft

labels in the discriminator; adding Gaussian noise to the discriminator inputs; inserting random noise to convolutional layers; and applying Leaky ReLUs as activation functions in the discriminators and generations. With these changes to the original CycleGAN baseline, we achieved stable generator outputs after approximately 15 training epochs.

## 4.2. Conditional CycleGAN Implementation

As an extension of our binary CycleGAN model, we next experiment with a conditional CycleGAN. We design this model to contain three class: low, medium, and high consumption classes, with the monthly consumption ranges given in the Data section. This conditional CycleGAN is similar to other multiclass CycleGAN such as StarGAN [2]; however, a key differentiation is that we tune our conditional CycleGAN for image translation in a continuous space with flexible class definitions. In previous conditional CycleGANs, the hard definitions are used for class distinctions e.g. a horse vs a zebra vs a lion. In our case, class definitions are soft, meaning that the user can specify binning thresholds for a high, medium and low electricity consumption classes.

The three-class conditional CycleGAN (hereafter, TricycleGAN) model uses the same architecture as the binary CycleGAN with one important change: along with the input images ( $x, y, z$ ), the model takes in a label that represents the desired class of the transformed image. For instance, image  $x$  would be paired with labels  $n_y$  or  $n_z$ , indicating that  $x$  should be transformed into either  $y_{fake}$  or  $z_{fake}$ . Identical to the binary CycleGAN, only two generators are required for the three different cycles: an  $G_{up}$  generator that transforms an image from a lower consumption class to a class with higher consumption one, and a  $F_{down}$  generator that performs the opposite transformation. This architecture is supported by the intuition that same-direction transformations will apply set of similar changes to varying degrees. For instance, transforming from class  $X$  to  $Y$  will likely emphasize larger road and building footprints, although to a lesser degree than in a transformation from class  $X$  to  $Z$ . Therefore, we thought it appropriate that these the generator weights be shared among cycles. Similarly, the TricycleGAN uses 2 discriminators, one for the lower consumption class and one for the higher consumption class in each transformation, as we believe the characteristics of what makes a transformed image real or fake can be shared across classes. Figure 2 shows the architecture of our TricycleGAN, which takes into account the label inputs. In designing our TricycleGAN implementation to closely resemble that of the binary CycleGAN, we create a model that scales with multiple classes, avoiding the increased computational requirements of training additional generator-discriminator pairs for each additional image-transformation cycle.

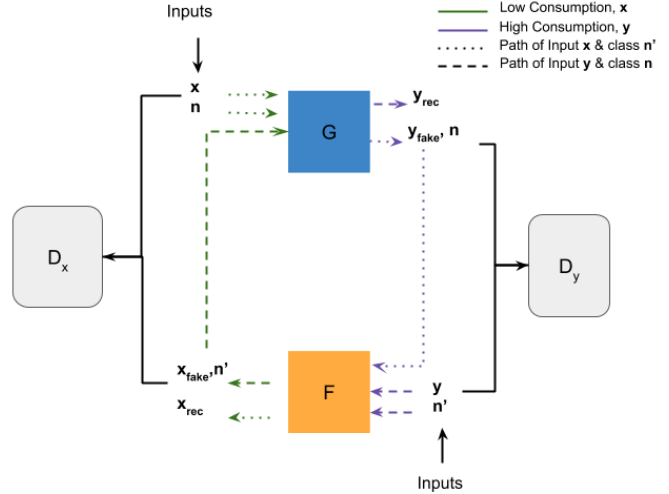


Figure 2: Conditional CycleGAN (TricycleGAN) architecture. The TricycleGAN architecture closely resembles that of the binary CycleGAN, although the desired image transformation cycle is specified by the additional inputs  $n$  and  $n'$ .

## 4.3. Electricity Consumption Classification Network

By subtracting the binary CycleGAN-generated images from their corresponding input images, we create a database of masks that transform images from one class to the next. We then experiment with classifying these masks in order to determine what level of binary classification accuracy (low or high) could be achieved if we only used the mask transformation as inputs and compared these results to two baselines: one that uses raw satellite imagery as training data, and another other that does the same with nighttime light measurements. As this classification task resulted in accuracies much higher than any we had been able to achieve with either baseline classifier, we initialized a simple UNet architecture that would transform a satellite image into a mask containing features that encode the information necessary to transition between classes. After training the UNet to recreate this set of transformation masks, either the output of the UNet, a image mask with the same spatial dimensions as the input image, or the feature space representation of the input image, taken after the last convolution layer in the network, is fed into a multilayer perceptron (MLP) for classification (we tested both methods to determine relative efficacy). With the UNet weights held constant, the multilayer perceptron is trained using a simple cross entropy loss between the actual and predicted image class labels. Figure 3 presents this network architecture.

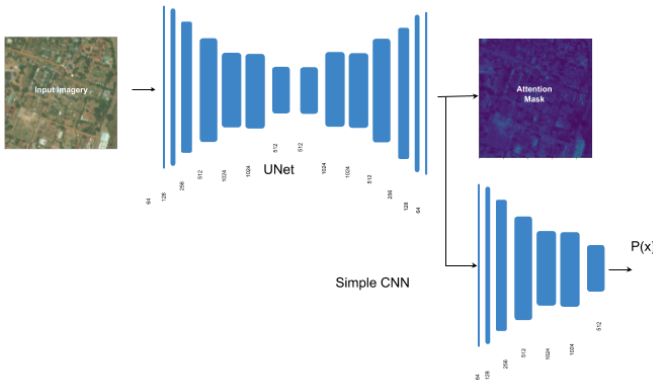


Figure 3: UNet and Simple CNN Architecture. The UNet is trained to recreate the attention masks generated by the binary CycleGAN; the recreated UNet masks and consumption class labels are then used as inputs to train a multilevel perceptron.

## 5. Results

### 5.1. Binary CycleGAN

Figure 4 presents the results from our binary CycleGAN implementation. In transitioning from a low-consumption image to a high-consumption one (top set of images), the CycleGAN implements two primary changes: road and building footprints are both enlarged and brightened. These changes have the effect of making roads and buildings stand in sharper contrast to background features. We believe these results make intuitive sense, as the lighter roads in the transformed images look to have a higher quality than roads in the original one, indicating more development in the generated image, which usually corresponds to higher electricity consumption. Similarly, tin roofs are typically seen as higher-status home improvements, and making the upgrade from a thatched roof to a reflective one likely parallels an increase in electricity consumption for a particular household. A secondary change visible in transforming from low-consumption to high-consumption is an increase in contrast in green areas surrounding houses, roads, and various other human developments. This increase in contrast has the effect of making cropland delineations in a larger pastoral area more clear, giving the impression of higher level of agricultural cultivation. Again, we find it realistic that more visible signs of development coincide with higher levels of electricity consumption. Transforming from the high consumption class to the low consumption class (bottom set of images) largely makes the inverse changes to the input imagery: road and buildings footprints are dimmed and made to blend in with their surroundings. These generated images on average look more rural than their high-consumption counterparts.

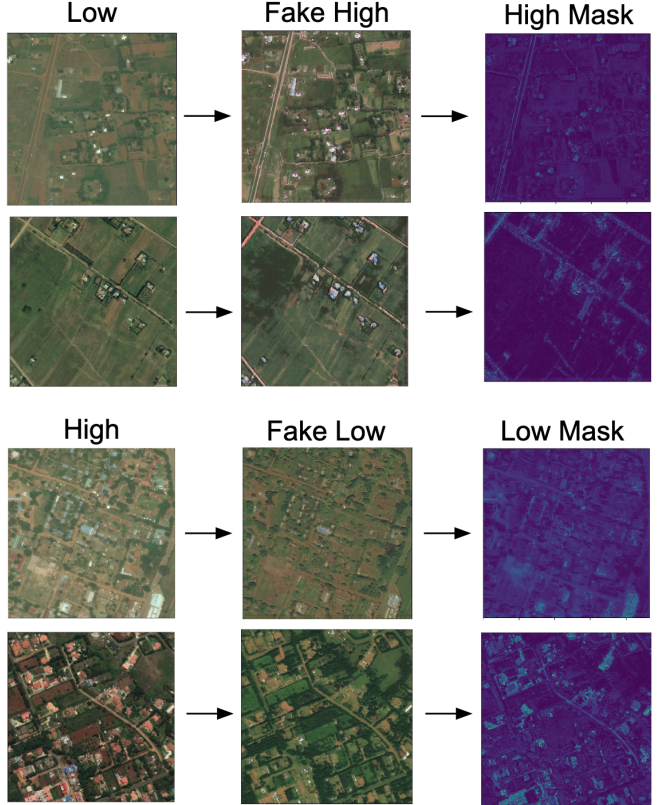


Figure 4: Results from the binary CycleGAN. The first set of transformations take a low-consumption image and transform it into a high-consumption image; the second set of image does the inverse. Left to right, the columns indicate the original image, the transformed image, and the absolute value of the transformed image minus the original image.

The third column in each binary CycleGAN transformation presented in Figure 4 shows the grayscale difference between the input and output images. The features present in these masks represent how specific features in an input image must change once it undergoes a class-transformation; as such, they contain the clearest insight into what image characteristics are important in making a classification decision about electricity consumption. Importantly, these changes are local in nature and do not occur on an image-wide scale: our model does not transform between image classes by increasing or decreasing an image's overall green hue, instead making specific adjustments to particular features in the image input.

### 5.2. Conditional CycleGAN

Results for our conditional CycleGAN – the TricycleGAN – exhibit similar image transformations to those generated by the binary CycleGAN. Figure 5 shows these transformed images: a pink border indicates the input im-

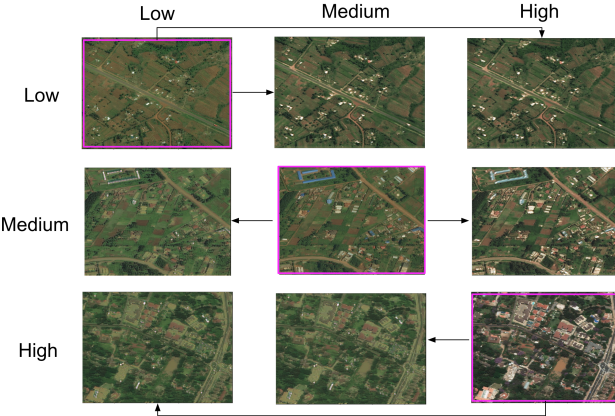


Figure 5: Conditional CycleGAN results. Images with a pink boundary indicate the original input image; arrows from this input image indicate the generated image in the desired output class.

age, and black arrows show the direction of the conditional transformation. On the up transformations, road and building footprints are enlarged and brightened; down transformations dim the same features. Comparing the up and down transformations of medium consumption images shows these differences most clearly: generated high-consumption images display more development and features more consistent with those in urban settings, while generated low-consumption images present the opposite. Unfortunately, our results for same-direction transformation are not as differentiable. There seems to be little difference between medium-consumption images and a high-consumption images if both images are generated from a low-consumption input; the same hold for down transformations. There are a couple possible reasons why these same-direction transformations aren't as instructive as the binary transformations. For one, there is significant visual similarity between periurban settings (generally with residential electricity consumption quantities in line with those for the medium-consumption class) and urban ones (with consumption in line with estimates for the high-consumption class), making it difficult for the TricycleGAN model to extract a third consumption class with unique feature identifiers. Relatedly, our set of training images may be too small to cleanly define distinctive transformations among all three classes. We further experimented with introducing the conditional label at multiple convolutional layers in our TricycleGAN under the assumption that a lone signal may get lost in the generation process, although results from this test were inconclusive as well.

### 5.3. Electricity Consumption Classification

Given the clarity of features presented in the binary CycleGAN masks, we hoped that recreating masks from an in-

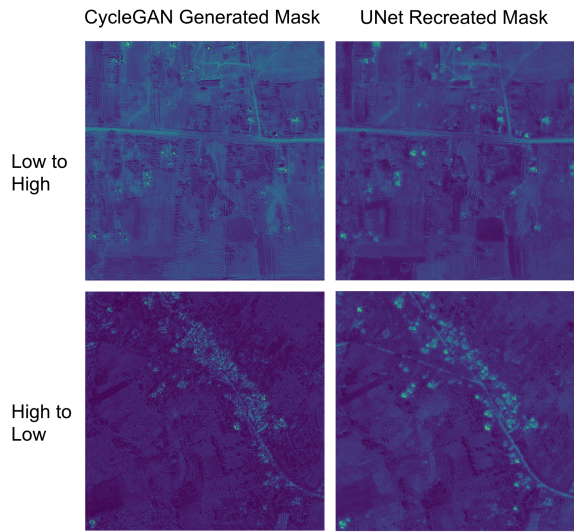


Figure 6: Mask Comparisons. Columns show the 1) CycleGAN generated masks and 2) the UNet recreated masks; rows present the mask results for the 1) low-to-high class transformation and 2) high-to-low class transformation.

put image and a learned UNet architecture would allow for high accuracy in our electricity consumption classification network. Over 120 training epochs, we attained a maximum classification accuracy using the mask recreation network of 0.74; we were not able to outperform daytime image and nighttime light classification baselines that respectively achieved accuracies of 0.77 and 0.75, each with an identical MLPs and training strategy. Changing the amount of images used to train the UNet mask generator had no effect on the performance of the classifier, indicating that there is a ceiling on the performance of the mask generator and that it can be achieved with a minimum of 30% of the training data. Neither stacking the UNet masks the satellite images nor coupling the masks with the nighttime lights measurements resulted in a greater increase in accuracy.

Figure 6 presents example CycleGAN and UNet masks: as these two types of masks look highly similar in both examples, yet the sets of images achieve training accuracies of 0.95 and 0.74 respectively, we conclude that there must be some information encoded in the binary CycleGAN transformations that cannot be recreated using the trained UNet. This information likely comes from the binary CycleGAN knowing which unique generator to place the image into given the image's label. Our results lend credence to the idea that there is a threshold around 0.75 that a classifier can achieve with satellite imagery, utility-reported residential electricity consumption data, and a CycleGAN architecture. Our results also indicate that it is likely that the CycleGAN modifies the same image features in its transformations that a MLP extracts during classification of satellite

imagery.

## 6. Conclusions

This report presents multiple methods of using satellite imagery and computer vision to explain residential electricity consumption in Kenya; as best we can tell, we present the first application of generative adversarial networks to the topics of understanding and predicting electricity consumption levels. Initially, we develop a binary CycleGAN that learns transformations between a low consumption class with monthly residential electricity consumption between 3 kWh/month and 30 kWh/month, and a high consumption class with monthly consumption between 90 kWh/month and 1000 kWh/month. Results from this first experiment reveal that the image transformations focus on altering building and road footprints in transitioning between image classes: in generating high consumption images, roads and buildings are brightened and enlarged; these same features are dimmed when generating low consumption images. Intuitively, these results indicate that more visible forms of development coincide with increased levels of electricity consumption. Roads with a higher amount of contrast to their surroundings typically indicate higher road quality, while more reflective buildings are representative of transitions from thatched roofs to tin ones; these findings dovetail with on-the-ground experiences about how sub-Saharan settings change with economic growth, development that also corresponds to higher electricity consumption. Compared to an approach that answers this question by analyzing classification heatmaps from a multilevel perceptron that discriminates between two levels of electricity consumption, a strategy which would only highlight the portions of an image that are important in making a classification decision, our generative approach visually presents exactly what feature transformations are required in transforming between classes.

Unfortunately, results for our conditional model are less conclusive. Our TricycleGAN has trouble differentiating between same-direction transformations, i.e. transforming a low-consumption image into a medium-consumption class by giving the network one target label and transforming the same image into a high-consumption class by giving the network a different label. We believe reasons for this model performance include high levels of visual similarity between images in periurban and urban settings that makes distinction between the medium-consumption and high-consumption classes difficult; we also think we lack the necessary training data for this more-challenging image transformation problem.

We also came to the conclusion that using recreated masks from the binary CycleGAN would not allow us to achieve an increase in electricity consumption classification performance. We acquired these recreated masks by

subtracting input images from their transformed outputs to train a UNet that extracts relevant class-transformation features from unseen satellite imagery; using the extracted features, we then train a multilevel perceptron on the binary classification task of predicting high or low electricity consumption. Our recreated mask-trained network is able to reach a similar level of performance – but not improve upon – two baseline classifiers that use either raw satellite imagery or nighttime light measurements. We attribute similar performances among the baseline satellite imagery network and our recreated mask network to the fact that both architectures likely use the same road and building features for classification.

Going forward, it remains an open question about what increases in electricity consumption prediction performance we are able to achieve using only satellite imagery. In inspecting our training data, we regularly encounter images which have visual features inconsistent with that image’s consumption class; for instance, a number of highly rural settings contain one or two buildings that place corresponding images in a high consumption class, even though a feature-based classification places these image in a low-consumption bin with other images they more closely resemble. Our next approach will likely involve semi-supervised learning of intermediary tasks for electricity consumption prediction using additional data sources, such as labeled building and road footprints as specified by Open Street Map. By explicitly learning these features before training a feature classifier, we will disconnect the feature learning from any built-in information regarding the image class, as was the case in our binary CycleGAN mask recreation. Moreover, we are skeptical about using generated images to help with classification. Generated images can help a network become more generalizable, as additional images will expand the distribution of model inputs; given the already wide distribution of satellite images and corresponding consumption values, we don’t believe this will be a problem for future classifiers we develop.

## 7. Acknowledgements

We would like to thank Professors Carl Vondrick, Jay Taneja, and Vijay Modi for all their help throughout this process. Professor Vondrick provided invaluable guidance about how to start the project, including by pointing us to the original CycleGAN paper, and helped recommend further avenues for exploration, specifically recommending that we implement a conditional variation of our original model. Professor Taneja helped answer various technical questions we had regarding implementation of our CycleGAN model and supplied important context about the goals of the project. Professor Modi supported us in his lab throughout the semester, funding and directing our efforts.

All code for this project is available at

[http://github.com/nsutezo/satellite\\_imagery\\_visualization](http://github.com/nsutezo/satellite_imagery_visualization).

## References

- [1] R. Caruana. Multitask learning. *Machine Learning*, 2007. 1
- [2] Y. Choi, M. Choi, M. Kim, J. Ha, S. Kim, and J. Choo. Stargan: Unified generative adversarial networks for multi-domain image-to-image translation. *CoRR*, abs/1711.09020, 2017. 4
- [3] C. N. Doll, J.-P. Muller, and J. G. Morely. Mapping regional economic activity from night-time light satellite imagery. *Ecological Economics*, 2005. 2
- [4] S. Fobi, V. Deshpande, S. Ondiek, V. Modi, and J. Taneja. A longitudinal study of electricity consumption growth in kenya. *Energy Policy*, 123:569 – 578, 2018. 1
- [5] I. J. Goodfellow, J. Pouget-Abadie, M. Mirza, B. Xu, D. Warde-Farley, S. Ozair, A. Courville, and Y. Bengio. Generative Adversarial Networks. *arXiv e-prints*, page arXiv:1406.2661, Jun 2014. 1
- [6] P. Isola, J. Zhu, T. Zhou, and A. A. Efros. Image-to-image translation with conditional adversarial networks. *CoRR*, abs/1611.07004, 2016. 2
- [7] Meyer. Silicon valley’s new spy satellites. *The Atlantic*, 2014. 1
- [8] M. Mirza and S. Osindero. Conditional generative adversarial nets. *CoRR*, abs/1411.1784, 2014. 2
- [9] M. X. W. M. D. D. B. L. S. E. Neal Jean, Marshall Burke. Combining satellite imagery and machine learning to predict poverty. *Journal of Science*, 353(6301):790 –794, 2016. 2
- [10] I. Nygaard, K. Rasmussen, J. Badger, T. Nielsen, L. Hansen, S. Stisen, S. Larsen, A. Mariko, and I. Togola. Using modeling, satellite images and existing global datasets for rapid preliminary assessments of renewable energy resources: The case of mali. *Renewable and Sustainable Energy Reviews*, 14(8):2359-2371, 2010, 2010. 1
- [11] A. Perez, S. Ganguli, S. Ermon, G. Azzari, M. Burke, and D. B. Lobell. Semi-supervised multitask learning on multispectral satellite images using wasserstein generative adversarial networks (gans) for predicting poverty. *CoRR*, abs/1902.11110, 2019. 2
- [12] K. Roth, A. Lucchi, S. Nowozin, and T. Hofmann. Stabilizing training of generative adversarial networks through regularization. *CoRR*, abs/1705.09367, 2017. 2
- [13] Safyan. Overview of the planet labs constellation of earth imaging satellites. 2015. 2
- [14] T. Salimans, I. J. Goodfellow, W. Zaremba, V. Cheung, A. Radford, and X. Chen. Improved techniques for training gans. *CoRR*, abs/1606.03498, 2016. 2
- [15] P. Samangouei, A. Saeedi, L. Nakagawa, and N. Silberman. Explaingan: Model explanation via decision boundary crossing transformations. September 2018. 2
- [16] P. Sutton and R. Costanza. Global estimates of market and non-market values derived from nighttime satellite imagery, land cover, and ecosystem service valuation. *Ecological Economics*, 41(3):509-527, 2002. 1
- [17] J. Zhu, T. Park, P. Isola, and A. A. Efros. Unpaired image-to-image translation using cycle-consistent adversarial networks. *CoRR*, abs/1703.10593, 2017. 1, 2, 3